

Production Decline Curves for Low-Pressure Gas Reservoirs Undergoing Simultaneous Water Production

Shahab Mohaghegh, SPE, and H.I. Bilgesu, SPE, West Virginia U., Turgay Ertekin, SPE, Penn State U.

Summary

A family of production decline curves for low-pressure gas reservoirs are presented for radial flow geometry with closed outer boundary and with a centrally located well. The proposed production decline curves are applicable to conventional gas reservoirs that produce gas and water simultaneously. The proposed decline curves exhibit unique characteristics for a variety of reservoir and fluid properties and pressure specifications at the well. The performance of the proposed decline curves were investigated against two different numerical simulators, and they were found to be capable of predicting the production of conventional gas reservoirs under two-phase flow conditions with good accuracy.

The decline curves presented in this paper have the potential of providing a practical tool by which production performance of gas reservoirs under two-phase flow conditions can be predicted for pragmatic purposes without using sophisticated numerical models.

Introduction

To formulate long-term economic predictions related to gas reservoirs, it is necessary to predict the long-term withdrawal rates physically possible for each well.¹ Rate/time decline curve extrapolation is one of the more often used tools of petroleum engineering. For a long period of time, various decline methods were regarded as empirical and not scientific. A new direction of decline curve analysis was introduced by Slider.² He developed an overlay method to analyze rate/time data. This method is similar to the log-log type-curve matching procedure used to analyze pressure-buildup and -drawdown data.³ This paper provides a type-curve approach to analyze production decline characteristics of gas reservoirs that produce water and gas simultaneously.

A large number of gas reservoirs are wet sands, and coproduction of gas and water takes place. Such reservoirs can be found in the Midwest and North Eastern U.S. (two-phase flow in these reservoirs is more significant during the early stages of the production), and in gas fields of the Middle East. Some gas fields in Europe have also reported water production. There are situations where initial water saturation is less than the critical water saturation of the formation, and the water does not flow. To take the presence of water phase into consideration, one needs to decrease formation porosity by subtracting the portion of the PV occupied by the immobile water phase. In most of the wet sands, however, initial water saturation exceeds the formation critical water saturation, and water becomes a dynamic phase and is produced simultaneously with gas. Under these conditions, treatment of a two-phase gas reservoir similar to a single-phase gas reservoir will generate erroneous results.

In a two-phase gas reservoir, relative permeability characteristics of the formation control the flow of fluids through the formation. Therefore, a dry sand reservoir and a wet sand reservoir with similar properties exhibit different production and depletion characteristics. Petroleum engineering literature contains production decline curves generated for single-phase gas reservoirs.⁴ These decline curves can be used in studying the production performance of gas reservoirs that are experiencing single-phase flow conditions. The use of these production decline curves to predict the performance of gas reservoirs undergoing two-phase flow conditions will lead to overestimation of the capabilities of the field in hand. The purpose

of this study is to provide a practical tool by which performance prediction and reservoir characterization of the wet gas sands can be achieved with good accuracy.

Formulation

To identify the dimensionless groups necessary in generating the decline curves, gas and water equations need to be expressed in a convenient form. In this development, invoking the procedure suggested by Al-Khalifah *et al.*⁵ to two-phase, gas/water reservoirs, equations are combined into a single expression. The gas and water transport equations in radial flow geometry are

$$\frac{1}{r} \frac{\partial}{\partial r} \left[r \frac{kk_{rg}}{\mu_g B_g} \frac{\partial p}{\partial r} \right] = \frac{\partial}{\partial t} \left[\frac{\phi S_g}{B_g} \right] \dots \dots \dots (1)$$

$$\text{and } \frac{1}{r} \frac{\partial}{\partial r} \left[r \frac{kk_{rw}}{\mu_w B_w} \frac{\partial p}{\partial r} \right] = \frac{\partial}{\partial t} \left[\frac{\phi S_w}{B_w} \right] \dots \dots \dots (2)$$

Consider a finite reservoir with no flow outer boundary specification. The production well is located at the center of the formation and produced at a constant pressure. The standard well test analysis assumptions are assumed to be in place in this development.

Multiplying Eq. 1 by B_g and Eq. 2 by B_w one obtains

$$\frac{B_g}{r} \frac{\partial}{\partial r} \left[r \frac{kk_{rg}}{\mu_g B_g} \frac{\partial p}{\partial r} \right] = B_g \frac{\partial}{\partial t} \left[\frac{\phi S_g}{B_g} \right] \dots \dots \dots (3)$$

$$\text{and } \frac{B_w}{r} \frac{\partial}{\partial r} \left[r \frac{kk_{rw}}{\mu_w B_w} \frac{\partial p}{\partial r} \right] = B_w \frac{\partial}{\partial t} \left[\frac{\phi S_w}{B_w} \right] \dots \dots \dots (4)$$

Addition of Eqs. 3 and 4 gives

$$\frac{B_g}{r} \frac{\partial}{\partial r} \left[r \frac{\lambda_g}{B_g} \frac{\partial p}{\partial r} \right] + \frac{B_w}{r} \frac{\partial}{\partial r} \left[r \frac{\lambda_w}{B_w} \frac{\partial p}{\partial r} \right] = B_g \frac{\partial}{\partial t} \left[\frac{\phi S_g}{B_g} \right] + B_w \frac{\partial}{\partial t} \left[\frac{\phi S_w}{B_w} \right], \dots \dots \dots (5)$$

$$\text{where } \lambda_g = \frac{kk_{rg}}{\mu_g} \dots \dots \dots (6)$$

$$\text{and } \lambda_w = \frac{kk_{rw}}{\mu_w} \dots \dots \dots (7)$$

Expanding the right side of Eq. 5 gives

$$\begin{aligned} RHS = & \phi B_g \left[\frac{1}{B_g} \frac{\partial S_g}{\partial p} - \frac{S_g}{B_g^2} \frac{\partial B_g}{\partial p} \right] \frac{\partial p}{\partial t} \\ & + \phi B_w \left[\frac{1}{B_w} \frac{\partial S_w}{\partial p} - \frac{S_w}{B_w^2} \frac{\partial B_w}{\partial p} \right] \frac{\partial p}{\partial t} \dots \dots \dots (8) \end{aligned}$$

Further simplification of Eq. 8 gives

$$RHS = \phi \left[\frac{\partial S_g}{\partial p} - \frac{S_g}{B_g} \frac{\partial B_g}{\partial p} + \frac{\partial S_w}{\partial p} - \frac{S_w}{B_w} \frac{\partial B_w}{\partial p} \right] \frac{\partial p}{\partial t} \dots \dots \dots (9)$$

$$\text{Because } S_g + S_w = 1.0, \dots \dots \dots (10)$$

it follows that

$$\frac{\partial S_g}{\partial p} + \frac{\partial S_w}{\partial p} = 0. \dots \dots \dots (11)$$

Substitution of Eq. 11 into Eq. 9 simplifies Eq. 9 further such that

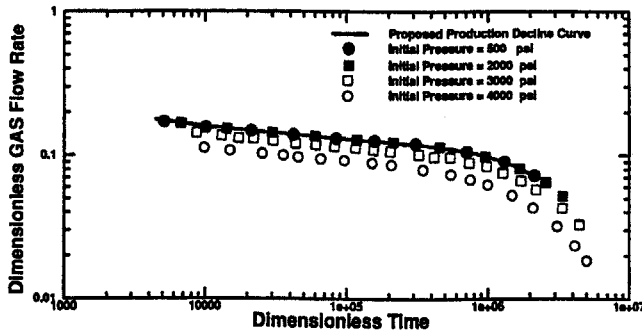


Fig. 1—Sensitivity of the proposed decline curves to initial reservoir pressure.

$$RHS = \phi c_i \frac{\partial p}{\partial t}, \dots \dots \dots (12)$$

$$\text{where } c_i = -\frac{S_g}{B_g} \frac{\partial B_g}{\partial p} - \frac{S_w}{B_w} \frac{\partial B_w}{\partial p}, \dots \dots \dots (13)$$

Using Eq. 12 in Eq. 5, one can write

$$\frac{B_g}{r} \frac{\partial}{\partial r} \left[r \frac{\lambda_g}{B_g} \frac{\partial p}{\partial r} \right] + \frac{B_w}{r} \frac{\partial}{\partial r} \left[r \frac{\lambda_w}{B_w} \frac{\partial p}{\partial r} \right] = \phi c_i \frac{\partial p}{\partial t}, \dots \dots \dots (14)$$

When the left side of Eq. 14 is expanded, one obtains

$$\lambda_g \frac{\partial^2 p}{\partial r^2} + B_g \frac{\partial}{\partial r} \left(\frac{\lambda_g}{B_g} \right) \frac{\partial p}{\partial r} + \frac{1}{r} \lambda_g \frac{\partial p}{\partial r} + \lambda_w \frac{\partial^2 p}{\partial r^2} + B_w \frac{\partial}{\partial r} \left(\frac{\lambda_w}{B_w} \right) \frac{\partial p}{\partial r} + \frac{1}{r} \lambda_w \frac{\partial p}{\partial r} = \phi c_i \frac{\partial p}{\partial t}, \dots \dots \dots (15)$$

Using the chain rule, one can write

$$\frac{\partial}{\partial r} \left(\frac{\lambda_g}{B_g} \right) \frac{\partial p}{\partial r} = \frac{\partial}{\partial p} \left(\frac{\lambda_g}{B_g} \right) \left(\frac{\partial p}{\partial r} \right)^2, \dots \dots \dots (16)$$

With the assumption of small pressure gradients and neglecting the squared terms, Eq. 15 reduces to

$$\frac{\partial^2 p}{\partial r^2} + \frac{1}{r} \frac{\partial p}{\partial r} = \frac{\phi c_i}{\lambda_i} \frac{\partial p}{\partial t}, \dots \dots \dots (17)$$

Eq. 17 can also be written as

$$\frac{1}{r} \frac{\partial}{\partial r} \left(r \frac{\partial p}{\partial r} \right) = \frac{\phi c_i}{\lambda_i} \frac{\partial p}{\partial t}, \dots \dots \dots (18)$$

In Eqs. 17 and 18, λ_i is defined as

$$\lambda_i = \lambda_g + \lambda_w, \dots \dots \dots (19)$$

At this point, gas and water transport equations describing two-phase flow conditions in a wet gas reservoir have been reduced to a single expression, which is analogous to the single-phase equation used in well test analysis. Transforming Eq. 18 into dimensionless form yields

$$\frac{1}{r_D} \frac{\partial}{\partial r_D} \left(r_D \frac{\partial \Delta p_D}{\partial r_D} \right) = \frac{\partial \Delta p_D}{\partial t_D}, \dots \dots \dots (20)$$

with customary dimensionless groups defined as

$$r_D = \frac{r}{r_w}, \dots \dots \dots (21)$$

$$\Delta p_D = \frac{p_i - p}{(p_i - p_w) q_D}, \dots \dots \dots (22)$$

$$t_D = \frac{2.637 \times 10^{-4} \lambda_i}{\phi c_i r_w^2} t, \dots \dots \dots (23)$$

$$\text{and } \left[q_D = \frac{q_{sc} B \mu}{2\pi k h (p_i - p_w)} \right]_{g,w}, \dots \dots \dots (24)$$

In the construction of the production decline curves, it is necessary to identify the dimensionless gas and water production rates together with the dimensionless time. From Eq. 24 one can deduce the dimensionless flow rate expressions for gas and water phases as

$$q_{Dg} = \frac{7.11 \times 10^5 q_{gsc} zT}{\lambda_g h p (p_i - p_w)}, \dots \dots \dots (25)$$

$$\text{and } q_{Dw} = \frac{141.2 q_{wsc} B_w}{\lambda_w h (p_i - p_w)}, \dots \dots \dots (26)$$

The constants in Eqs. 23, 25, and 26 imply the use of the field units for all the parameters.

Construction of the Proposed Decline Curves. To generate the proposed decline curves, as shown in the previous section, gas and water equations were put into a convenient form that describes two-phase flow in gas/water reservoirs. A two-phase, 1D, radial numerical simulator⁶ was used to generate flow rate vs. time data. The data generated by the numerical model were used to calculate the previously identified dimensionless time and dimensionless flow rate groups, which then were plotted on a log-log scale. All the pressure- and saturation-dependent parameters that appear in the dimensionless groups were evaluated at the initial pressure and initial saturation. The decline curves were generated for different sandface to initial formation pressure ratios as well as for different reservoir extent. It was observed that these decline curves performed better at initial formation pressures below 2,000 psi. Once the initial formation pressure exceeds 2,000 psi, the uniqueness and independency of the proposed decline curves to the pressure volume temperature (PVT) data become attenuated. Fig. 1 displays the proposed decline curve generated at different initial formation pressures for $p_w/p_i = 0.5$. It is clear that up to 2,000 psi the proposed decline curve displays unique characteristics and, as initial pressure increases, the uniqueness of the decline curve is increasingly compromised. This is expected because at relatively low pressures the product of the gas viscosity and compressibility factor is constant. As the pressure becomes higher, the constant nature of this functional group is compromised, and the uniqueness of the decline curves start to deteriorate.

Two separate production decline curves are generated for gas and water flow rates. Table 1 summarizes the parameters used in constructing these production decline curves. To generate the production decline curves at different p_w/p_i ratios, the initial pressure was kept constant and the wellbore pressure was changed accordingly. Fig. 2 displays the gas flow rate decline curves generated at different p_w/p_i ratios for different reservoir extent. Fig. 3 shows the corresponding water production decline curves.

Discussion of Results

Sensitivity Analysis. The performance of the proposed decline curves was investigated under a wide range of reservoir properties. From different reservoir parameters, dimensionless gas flow rate and dimensionless time groups were calculated at various times and were marked over the proposed decline curves. As it is clearly seen in Figs. 4 through 6, in every case a good match was achieved. These verification tests were conducted at $r_{eD} = 100$ to save computer time. Fig. 7 shows different relative permeability characteristics used to investi-

TABLE 1—RESERVOIR PARAMETERS USED TO GENERATE PROPOSED PRODUCTION DECLINE CURVES*	
Initial pressure, psi	1000
Bottomhole pressure, psi	500
Well radius, ft	0.5
Permeability, md	1
Porosity, %	10
Initial gas saturation, %	40
Formation thickness, ft	10
Gas gravity (air = 1.0)	0.6
Reservoir temperature, °R	530
Water viscosity, cp	0.9707

*For the relative permeability characteristics see Set A of Fig. 7.

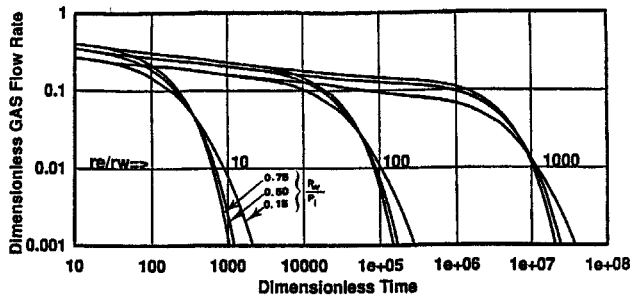


Fig. 2—Gas flow rate decline curves for gas reservoirs under two-phase flow conditions.

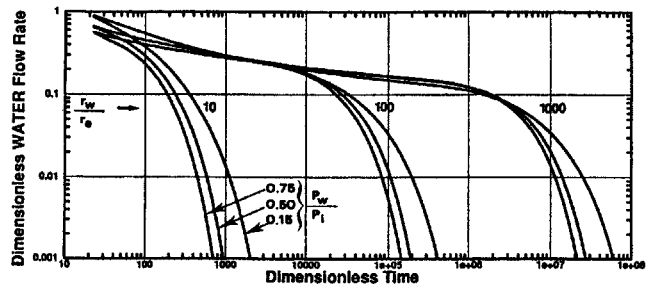


Fig. 3—Water flow rate decline curves for gas reservoirs under two-phase flow conditions.

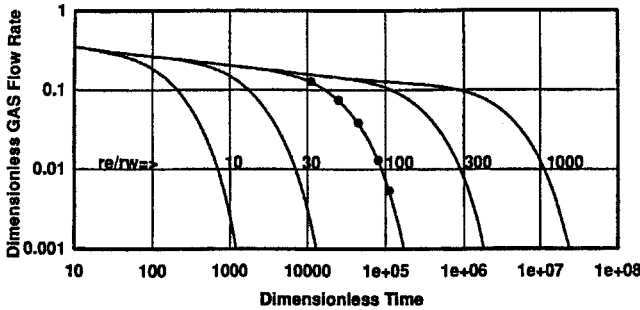


Fig. 4—Verification of the decline curves for a wet gas sand with following characteristics: $SG=0.6$, $p_i=1000$ psi, $p_w=500$ psi, $S_{gi}=40\%$, $f=10\%$, $k=0.01$ md, $h=10$ ft, $r_w=0.5$, $r_e=50$ ft.

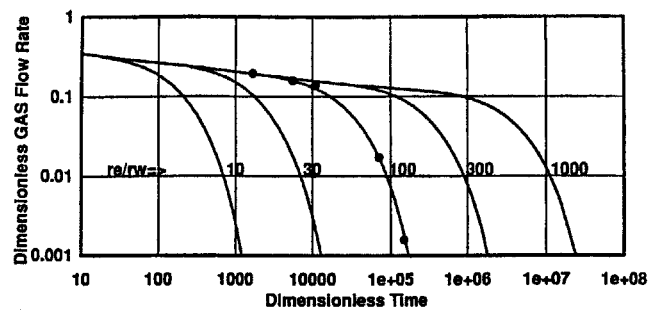


Fig. 5—Verification of the decline curves for a wet gas sand with following characteristics: $SG=0.6$, $p_i=1000$ psi, $p_w=500$ psi, $S_{gi}=50\%$, $f=15\%$, $k=0.15$ md, $h=10$ ft, $r_w=0.5$, $r_e=50$ ft.

gate the performance of the proposed decline curves when relative permeability characteristics of the reservoir are changed. The results of this investigation are shown in Fig. 8. The data points shown in Fig. 8 correspond to the same real times. From Fig. 8 it is clear that the characteristic nature of the decline curve is preserved successfully against a variety of relative permeability characteristics.

Tests Against Single-Phase Decline Curves. To demonstrate explicitly the need for a set of two-phase decline curves for conventional gas reservoirs, a test was conducted in which the performance of a single-phase production decline curve is compared with that of a two-phase production decline curve in predicting the gas flow rates from a particular formation. The parameters of Table 1 were used to construct these curves, and Fig. 9 displays the results of this comparison. As expected, the single-phase production decline curve predicts a higher gas flow rate than the two-phase production decline curve. The difference in the two predictions will vary according to the relative permeability characteristics of the formation. Obviously, as the mobility of the water in the formation increases, the prediction of the single-phase production decline curve becomes more unrealistic. The gas composition and calculation of dimensionless groups are shown in Appendix A.

Tests Against Different Numerical Simulators. The proposed decline curves were generated and subsequently tested using an in-

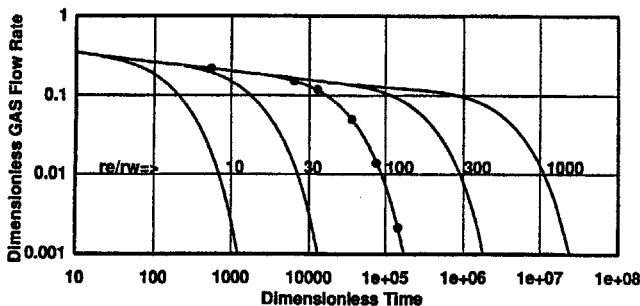


Fig. 6—Verification of the decline curves for a wet gas sand with following characteristics: $SG=0.6$, $p_i=2000$ psi, $p_w=1000$ psi, $S_{gi}=60\%$, $f=30\%$, $k=1.0$ md, $h=40$ ft, $r_w=0.5$, $r_e=50$ ft.

house numerical simulator. To test the uniqueness and applicability of the proposed decline curves further, more tests were conducted using two different sets of data in two different numerical models that were not instrumental in the construction of the decline curves. These tests were designed to discover whether the decline curves presented in this paper were biased toward the numerical model used in their construction. The numerical model used in the first test (Test 1) was a commercial simulator that uses IMPES procedure to solve the multiphase flow problems. The in-house numerical model used in the generation of the decline curves is a fully implicit model. Furthermore, the commercial numerical model uses Cartesian coordinates, while the in-house model uses radial coordinates. Table 2 represents the relative permeability data used in this test. Formation characteristics, which were input during the same test, are presented in Table 3. Fig. 10 shows the agreement between the simulated data and predictions from the two-phase decline curves for the gas production rate. Fig. 11 shows, for the same test, the agreement between the simulated data and the predicted water flow rates. Note that the anomalous behavior in the simulated data in Fig. 11 is caused by the relatively long timesteps used during the simulation.

In a separate test (Test 2), a new set of data was used on another commercial model.⁷ Relative permeability data as well as formation characteristics for this test are shown in Tables 2 and 3, respectively. In this test, two separate approaches were examined to demonstrate the different usages of the proposed curves. First a type-curve matching approach is tested. Using this technique, one may be able to use the production data for reservoir characterization purposes. Plotting the gas production data on the same scale as the type curves and overlapping for a match, a match point was obtained (Fig. 12). Using this match point ($q_{Dg}=0.3$, $t_D=1 \times 10^8$ and $q_g=0.7$ MMscf/D, $t=20,000$ days) the permeability of the reservoir is calculated, with Eq. 25, to be 0.74 md, while the actual permeability that was put into the simulator was 0.75 md. The porosity calculated from the type-curve matching procedure using Eq. 23 is 27.8%, and the input porosity to the simulator was 25%. This shows the ability of proposed curves in accurately characterizing gas reservoirs producing under two-phase (gas and water) flow conditions.

On a second approach in Test 2, it was attempted to predict the performance of a well producing from the center of the reservoir with known reservoir characteristics. Fig. 13 shows production data simulated by the simulator vs. those of decline curve prediction.

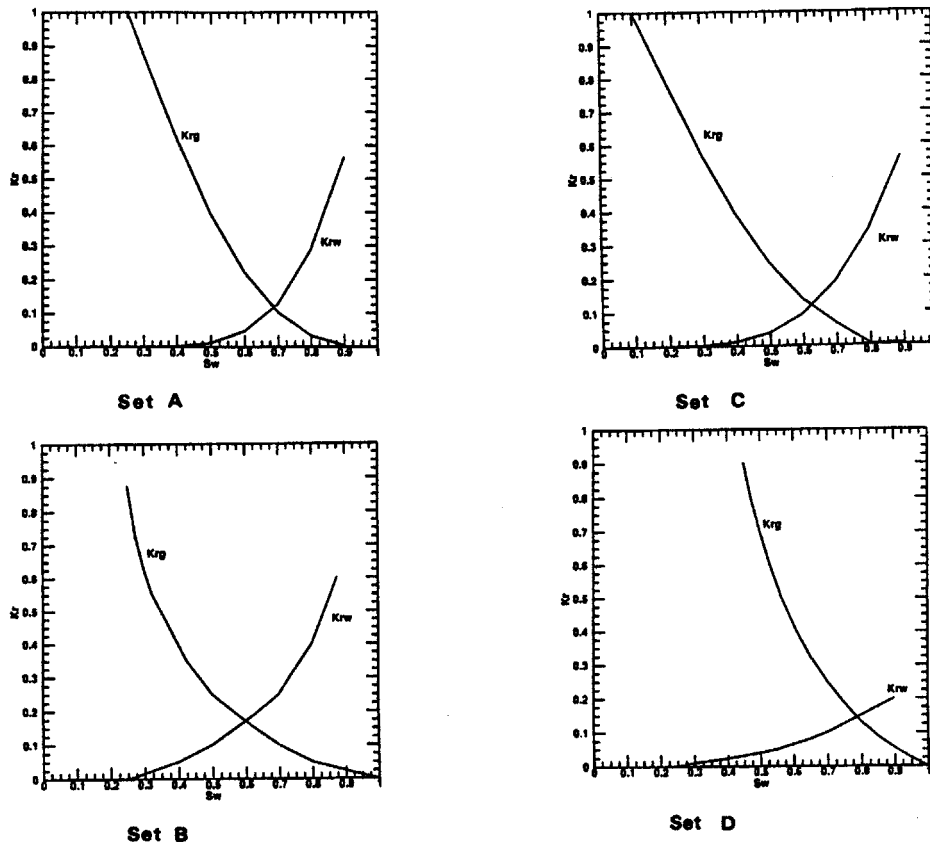


Fig. 7—Relative permeability characteristics used in testing the performance of the proposed decline curves.

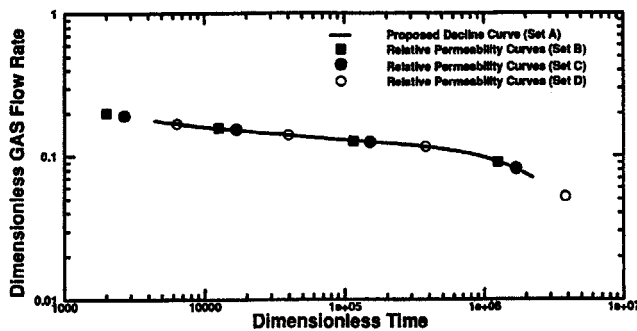


Fig. 8—Sensitivity of the proposed decline curves to relative permeability characteristics.

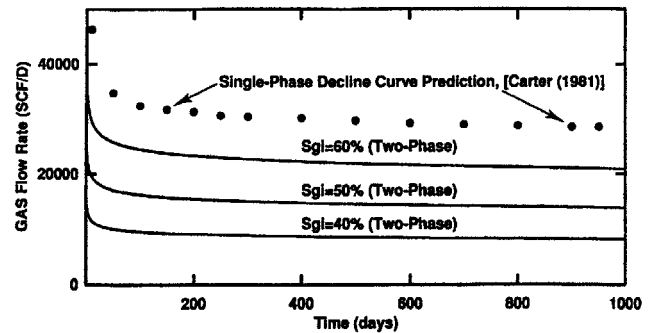


Fig. 9—Gas flow rate predictions obtained by single-phase and two-phase decline curves for a fixed set of reservoir parameters but with different initial gas saturations.

Conclusions

1. Our experimentation with the two-phase production decline curves indicates that the proposed curves provide a practical and powerful tool in predicting the performance of a low-pressure gas reservoir under two-phase flow.
2. A single expression representing water and gas flow in the reservoir was presented.
3. Dimensionless groups were identified, and the decline curves were constructed using a numerical simulator.
4. A wide range of reservoir properties were investigated to examine the unique and universal nature of the decline curves.
5. The proposed decline curves were tested against two different independent commercial numerical models. The results further proved the robustness of the proposed decline curves.

Nomenclature

- B = formation volume factor, L^3/L^3 , bbl/STB
 c = compressibility, L^2/m , psi^{-1}
 h = reservoir thickness, L, ft

- k = permeability, L^2 , md
 p = pressure, m/Lt^2 , psia
 q = flow rate, L^3/t , scf/D
 r = radius, L, ft
 S = saturation, fraction
 t = time, t, hr
 T = reservoir temperature, °R
 z = gas deviation factor, fraction
 λ = mobility, L^3/tm , md/cp
 μ = viscosity, m/Lt , cp
 ϕ = porosity, fraction

Subscripts

- D = dimensionless
 g = gas properties
 i = initial condition
 sc = standard condition
 t = total properties
 w = water properties

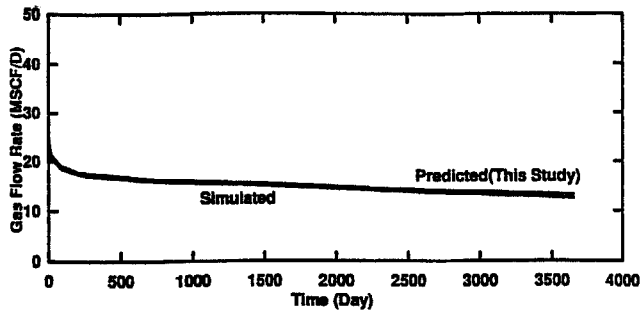


Fig. 10—Predicted gas flow rates from a numerical simulator and from the proposed decline curve.

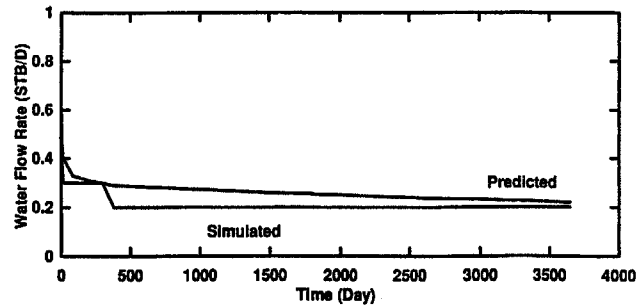


Fig. 11—Predicted water flow rates from a numerical simulator and from the proposed decline curve.

S_w	k_{rw} (Test 1)	k_{rg} (Test 1)	k_{rw} (Test 2)	k_{rg} (Test 2)
0	0	1	0	1
0.15	0	1	0	1
0.216	0.01	0.667	0	0.78
0.33	0.09	0.545	0.09	0.66
0.4	0.13	0.486	0.15	0.6
0.47	0.227	0.433	0.22	0.475
0.53	0.377	0.393	0.27	0.375
0.58	0.531	0.264	0.32	0.32
0.62	0.669	0.143	0.37	0.28
0.67	0.734	0.074	0.425	0.245
0.69	0.8	0.012	0.485	0.24
0.92	0.95	0	0.875	0.018

Parameter	Test 1	Test 2
Initial pressure, psi	1,750	1,200
Well pressure, psi	800	360
Well radius, ft	0.4	0.5
Reservoir radius, ft	1500	500
Permeability, md	0.1	0.75
Porosity, %	7.5	25
Gas saturation, %	55	50
Thickness, ft	15	33

References

- Gurley, J.: "A Productivity and Economic Projection Method—Ohio Clinton Sand Gas Wells," *JPT* (Nov. 1963) 1183.
- Slider, H.C.: "A Simplified Method of Hyperbolic Decline Curve Analysis," *JPT* (March 1968) 235.
- Fetkovich, M.J.: "Decline Curve Analysis Using Type Curves," *JPT* (June 1980) 1065.
- Carter, R.D.: "Characteristic Behavior of Finite Radial and Linear Gas Flow Systems—Constant Terminal Pressure Case," paper SPE 9887 presented at the 1981 SPE Low Permeability Symposium, Denver, May 27–29.
- Al-Khalifah, A.-J.A., Aziz, K., and Horne, R.N.: "A New Approach to Multiphase Well Test Analysis," paper SPE 16743 presented at the 1987 SPE Annual Technical Conference and Exhibition, Dallas, Sept. 27–30.
- King, G.R., Ertekin, T., and Schwerer, F.C.: "Numerical Simulation of the Transient Behavior of Coal Seam Degassification Wells," *SPEFE* (April 1986) 165.
- ECLIPSE 100 Black Oil Simulator, Version 93A, Intera Information Technologies, Petroleum Production Div., Denver (1993).
- Mohaghegh, S.: "Pressure and Production Type-Curves as Applied to Wet-Gas Sands and Coal Seams," PhD dissertation, Pennsylvania State U., University Park, PA (1992).

Appendix A

Following is the gas composition used in determining the gas properties used in the reservoir simulator.

Component	Mole Fraction
CH ₄	0.9190
C ₂ H ₆	0.0630
C ₃ H ₈	0.0110
C ₄ H ₁₀ (n)	0.0029
CO ₂	0.0040
N ₂	0.0001

The specific gravity of the above gas is calculated to be 0.60.

Sample Calculation.⁸ Following is a sample calculation for dimensionless rate and dimensionless time. Reservoir and fluid properties are given in Table 4. The dimensionless rate and time are calculated at $t = 0.9$ days when reservoir is producing 10 MMscf/D.

First total mobility and total compressibility is calculated from the data in Table 4.

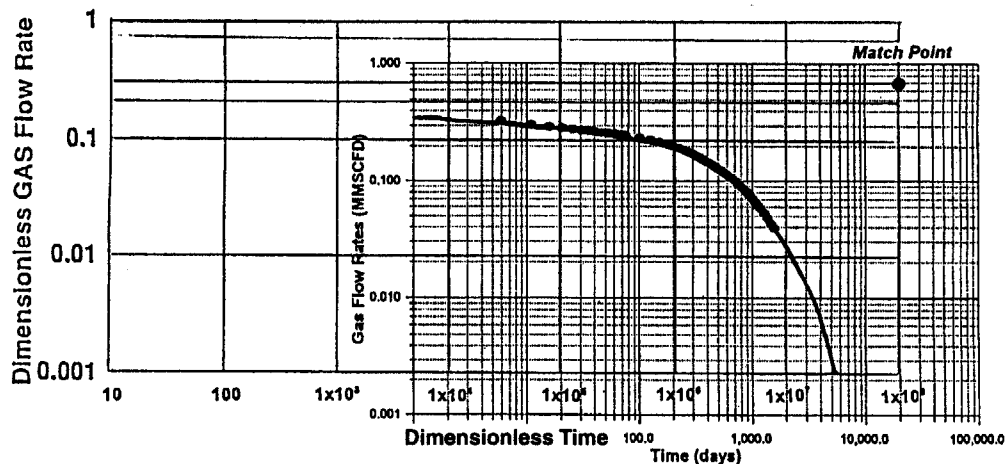


Fig. 12—Reservoir characterization by type-curve matching procedure using the proposed type curves.

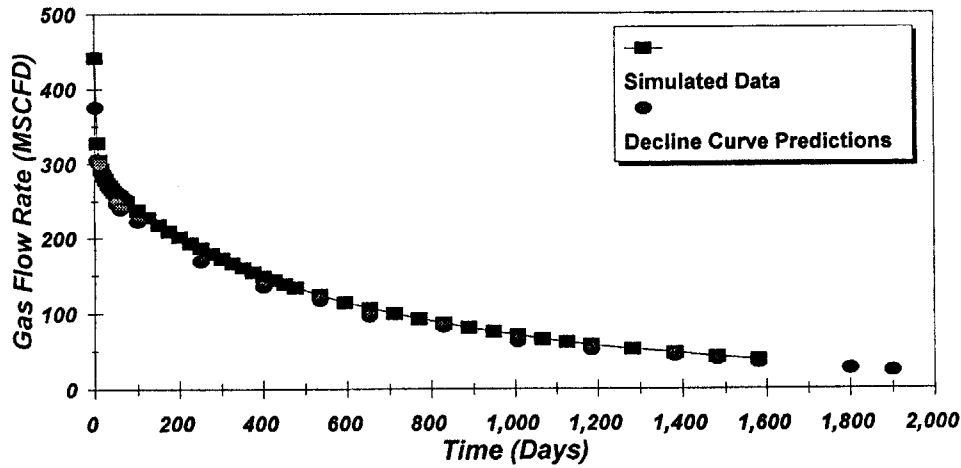


Fig. 13—Predicted gas flow rates from a commercial simulator⁸ and from the proposed decline curves.

TABLE 4—RESERVOIR AND FLUID PROPERTIES USED FOR CALCULATIONS IN APPENDIX A	
p_i , psi	1991
r_w , ft	0.5
S_{gi}	0.3
p_{wf} , psi	400
h , ft	85.6
Gas gravity	0.6
T , °R	530
μ_w , cp	1.0
μ_g , cp	0.01622
z_i	0.7995
k_{rg}	0.1024
k_{rw}	0.1296
k , md	22.4
ϕ	0.157
c_w , psi ⁻¹	5×10^{-6}

$$\lambda_g = \frac{kk_{rg}}{\mu_g} = \frac{(22.4)(0.1024)}{0.01622} = 141.415,$$

$$\lambda_w = \frac{kk_{rw}}{\mu_w} = \frac{(22.4)(0.1296)}{1.0} = 2.903,$$

$$\lambda_t = \lambda_g + \lambda_w = 144.318,$$

$$c_t = S_g c_g + S_w c_w,$$

$$\text{and } c_t = (0.30)\left(\frac{1}{1991}\right) + (0.7)(5 \times 10^{-6}) = 1.542 \times 10^{-4} \quad \text{..... (A-1)}$$

Using Eq. 25, dimensionless rate is calculated

$$q_{Dg} = \frac{(7.11 \times 10^5)(10)(0.7995)(530)}{(141.415)(85.6)(1991)(1991-400)} = 0.078,$$

and dimensionless time is calculated using Eq. 23,

$$t_D = \frac{(2.367 \times 10^{-4})(144.318)(0.9)(24)}{(0.157)(1.542 \times 10^{-4})(0.25)} = 1351819. \quad \text{..... (A-2)}$$

SI Metric Conversion Factors

bbl × 1.589873	E - 01 = m ³
cp × 1.0*	E + 00 = Pa · s
°F (°F - 32)/1.8	= °C
ft × 3.048*	E - 01 = m
ft ³ × 2.831685	E - 02 = m ³
in. × 2.54*	E + 00 = cm
psi × 6.894757	E + 00 = kPa
°R °R/1.8	= °K

*Conversion factor is exact.

SPEFE

Shahab Mohaghegh is an assistant professor of petroleum and natural gas engineering at West Virginia U., Morgantown. His research interests include reservoir characterization, application of petroleum engineering technology to environmental processes, and application of machine intelligence to energy and environmental sciences. He holds BS and MS degrees in natural gas engineering from Texas A&I U. and a PhD in petroleum and natural gas engineering from Pennsylvania State U. **H. Ilkin Bilgesu** is an assistant professor of petroleum and natural gas engineering at West Virginia U. Previously, he worked for the Turkish Petroleum Corp. and taught at South Dakota School of Mines and Technology. He holds a BS degree from Middle East Technical U. in petroleum engineering, an MS degree from the Colorado School of Mines in chemical and petroleum refining engineering, and a PhD degree in petroleum and natural gas engineering from Pennsylvania State U. He was a member of the program committee for the 1993 and 1991 SPE Eastern Regional Meetings. **Turgay Ertekin** is the Quentin E. and Louise L. Wood Professor and chairman of the Petroleum & Natural Gas Engineering Section at Pennsylvania State U., where he earned a PhD degree in petroleum and natural gas engineering. He holds BS and MS degrees in petroleum engineering from Middle East Technical U. Ertekin was 1993-94 Executive Editor for *SPE Formation Evaluation*, a 1990-93 ABET Program Evaluator, a 1990-92 Review Chairman, and a 1984-89 Technical Editor.



Mohaghegh



Bilgesu



Ertekin